Effect of Different SiCp Particle Sizes on the Behavior of AA 7075 Hot Deformation Composites Using Processing Maps

M. Rajamuthamilselvan, S. Rajakumar, and S. Kavitha

Abstract The mechanical reaction of 7075 Al alloy and Al 7075/15% SiCp with 5 μm, 20 μm, and 63 μm metal-matrix composites is investigated using a hot compression sample. In order to achieve the processing map of the studied material following the dynamic material model, the flow stress curves obtained in temperature ranges of 300–500 °C and strain rate ranges of 0.001–1.0 s-1, respectively. All flow instability zones are analyzed by an optical microscope. Microstructural characterization carried out using an optical microscope image analyzer on compressed composite specimens showed safe domains and non-safe domains. The composites of AA7075/20 μm SiCp showed higher efficiency, flow stress, and lower regimes of instability than alloy.

Keywords Mmcs · Processing maps · Dynamic recrystallization · Hot workability

1 Introduction

Hot deformation is an essential step in aluminum alloy production. Number of studies on the hot workability of these alloys has been carried out [1, 2]. Higher flow stress can be obtained for the alloy with unstable microstructure due to dynamic precipitation, and the flow curves often show significant softening due to subsequent coarsening of particles [1]. Due to their high mechanical properties and low density, the high-strength Al–Zn–Mg–Cu alloys were widely used in aeronautical structures. However,

M. Rajamuthamilselvan (✉)
Department of Mechanical Engineering, Government College of Engineering, Srirangam, Trichy, Tamilnadu 620012, India
e-mail: rajanarmi@yahoo.co.in

S. Rajakumar
Department of Manufacturing Engineering, Annamalai University, Annamlai Nagar, Chidambaram, Tamilnadu 608002, India

S. Kavitha
Department of Electronics and Instrumentation Engineering Annamalai University, Annamlai Nagar, Chidambaram, Tamilnadu 608002, India

G. Kumaresan et al. (eds.), *Advances in Materials Research*, Springer Proceedings in Materials 5, https://doi.org/10.1007/978-981-15-8319-3_123

due to the high concentration of Zn, Mg, and Cu elements, their hot workability is often reduced. Thus, to obtain only the required shape, but also more importantly the desired microstructure and properties, the hot deformation parameters need to be optimized. Because of the practical importance, the warm deformation behavior of some Al–Zn–Mg–Cu alloys [3] has been investigated.

Al-MMCs can substitute for steel to some degree when reinforced with ceramic particulate materials such as SiC, Al2O3, B4C, and TiC. Consequently, they have great potential of application in defense and automotive industries [4].The high-strength metal-matrix composites combine the high strength and hardness of the reinforcing phase with the ductility and toughness of light metals that the particulate-reinforced metal-matrix composites have emerged as attractive materials for use in a range of applications involving industry, military, and space-related applications [5]. The renewed interest in metal-matrix composites was encouraged by the production of reinforcement material that either offers improved properties or reduced costs compared to existing monolithic materials [6]. As a function of temperature, strain rate, and strain, the input to produce a processing map is the experimental flow stress information. Since the generated map will only be as good as the input data, it is important to use precise, reliable, and yet simple experimental technique to generate them [7].

Reinforcement of the size and volume fraction are two important factors controlling the mechanical properties of MMC. Clearly, the spacing between particles is an important geometric parameter to regulate an inhomogeneous plastic deformation in the composite. According to Liu et al.[8], the strain gradient can effectively describe this in homogenous plastic deformation. Comparative study on the effect of SiCp particle sizes and volume fraction on 7075 Al/SiCp composites deformation behavior is discussed below.

The processing map technique is based on the concept of dynamic materials, whose principles were mentioned earlier [9, 10]. In short, the work piece undergoing a hot deformation is considered to be a power dissipater, and the total power instantaneously dissipated is given by.

$$P = \int_0^{\acute{\epsilon}} \sigma . d\acute{\epsilon} + \int_0^{\sigma} \acute{\epsilon} . d\sigma = G + J \tag{1}$$

where there is the strength of flow and where there is the rate of stress. In terms of terminology of physical systems, the first integral is called G content representing heat deformation, and the second one is a J co-content representing microstructural dissipation, which is a complementary part of G content. The strain rate sensitivity (m) is the factor that divides energy between heat deformation and microstructural changes as follows:

$$\frac{dJ}{dG} = \frac{\acute{\epsilon} . d\sigma}{\sigma . d\acute{\epsilon}} = \frac{\acute{\epsilon}\sigma d \ln \sigma}{\sigma \acute{\epsilon} d \log \acute{\epsilon}} \approx \frac{\triangle \log \sigma}{\triangle \log \acute{\epsilon}} = m \tag{2}$$

The efficiency of power dissipation (η) which occurs during deformation by microstructural adjustments is derived by contrasting the nonlinear power dissipation which occurs instantaneously in the workpiece with that of a linear dissipater ($m = 1$).

$$\frac{\triangle J/\triangle P}{(\triangle J/\triangle P)linear} = \frac{m/(m+1)}{1/2} = \frac{m}{m+1} = \eta \tag{3}$$

The energy dissipation map represents the three-dimensional variance of temperature and strain efficiency that is generally viewed as a contour map of iso-efficiency. Furthermore, the extreme principles of irreversible thermodynamics applied to continuum mechanics of large plastic flow were explored to establish a criterion for the onset of flow instability provided by the parameter of instability ξ (έ)

$$\xi\left(\acute{\varepsilon}\right) = \frac{\delta \ln(m/m+1)}{\delta \ln \acute{\varepsilon}} + m < 0 \tag{4}$$

The variance of the parameter of instability as a function of temperature and stress level is a map of instability that delineates instability regimes where ξ is negative. A superimposition of the instability map on the energy dissipation map provides a processing map showing domains where individual microstructural processes dominate and limiting flow instability conditions for regimes. Processing maps help to identify hot working temperature–strain rate windows where the material's intrinsic workability is maximum (e.g., superplasticity or dynamic recrystallization (DRX)) and also prevent flow instability regimes (e.g., flow location or adiabatic shear bands) or cracking. Previously, the processing map technique was used to research the mechanisms of warm deformation in Al and its alloys [9, 11] including dynamic recrystallization (DRX) and flow instability.

The standard equation of the kinetic rate relative to the flow stress (σ) and the strain rate (έ) is given by [12, 13]:

$$\acute{\epsilon} = A\sigma^n \exp(-Q/RT) \tag{5}$$

where A = constant, n = stress exponent, Q = activation energy, and R = gas constant. The rate-controlling mechanisms are identified on the basis of the activation parameters n and Q.

2 Experimental Work

Stir-casting technique was used to produce 7075Al alloy, 7075 Al alloy with reinforcement size was 5 μm, 20 μm, and 63 μm SiCp with 15% silicon carbide composite volume fraction. The aluminum alloy matrix content was 7075. Using a revolving impeller in Argon setting, preheated SiCp (250° C) was applied to the melt

and mixed and poured in permanent mold. The cylindrical samples were made from the extruded rods, 10 mm in diameter and 10 mm in height. The hot compression tests were carried out on a universal testing machine controlled by 1OT servo for different strains (0.1–0.5), strain rates (0.001 s^{-1}–1.0 s^{-1}), and temperatures (300–500° C). The specimen's temperature was monitored using a chromel/alumel thermocouple embedded in a 0.5 mm hole drilled half of the specimen's height [14]. The samples were immediately quenched in water after compression analysis and microstructure were examined for the cross section. Specimens have been deformed to half of their original height. Parallel to the compression axis, deformed specimens were sectioned, and the cut surface was prepared for metallographic testing. Specimens have been etched with the solution from Keller [15]. The specimen microstructure was obtained through an optical microscope, and the deformation mechanism was studied. For different strain levels, temperatures at a constant strain of 0.5 were evaluated using the flow stress information, power dissipation efficiency, and flow instability. Processing maps for 7075 Al alloy and Al 7075/SiC/15 percent composites were produced for 0.5 strains.

3 Result and Discussions

3.1 Interpretation from Flow Curves

It is well known that mechanical performance also depends on the size of the reinforcement particle in particulate-reinforced metal-matrix composites. If the reinforcement particle size is larger, yield and flow stresses will be increased while the strength and ductility of the fracture will often be decreased. Therefore, reinforcement particles of large size have a high fracture propensity during low temperature deformation. This pattern may also tend to be at a moderately high temperature. In such a situation, under terms of flow pressure enhancement, the impact of additional reinforcement becomes less. Nonetheless, flow pressure is linear at high stress levels, indicating the effect of increased density of dislocation in the matrix [16].

Figure 1a–d shows the flow curves of 7075 aluminum alloy and 7075Al/15%SiCp composites deformed at 0.1 s^{-1} and different temperatures ranges from 300–500 °C, respectively. The materials flow stress increases as the stress rate increases and the temperature decreases. The typical behavior of warm working conditions deformed metals [17]. For the reinforced composites, the flow pressure is lower in all situations. In the curves, it is clearly observed that there is considerable softening of the flow in composites, especially at higher strain values. This shows that the variance in flow pressure with change in particle size for a constant 15 percent composite volume fraction. It is interesting to note that the flow pressure rises at 400° C with particle size, whereas at a higher deformation temperature of 450° C it shows a decreasing pattern. It is well known that enhancing the mechanical properties of hard ceramic particles in a soft metallic matrix [18]. Larger SiC particle size added in composites

shows higher strain durability index and lower strength coefficient values due to better SiC load transfer rate to the aluminum matrix compared to lower particle size [19]. Therefore, the flow pressure of composites increases with increased particle size of reinforcement. With increased size of SiCp of composites, the better densification increases.

Because of a steep rise in the same way as the particle size is finer; the fraction of smaller particles will create a high dislocation density relative to larger particles [20]. Due to this crucial variation in dislocation size, a large number would be generated locally in homogenous areas, which in turn would affect local flow behavior. This can lead to a non-uniform reduction in flow and flow stress, making the system plastically unstable. Experiments in which a steep increase in dislocation density is observed with a decrease in particle size can describe a critical size. An increase in particle size, on the other hand, reduced composite strength and increased ductility [21].

3.2 Interpretation from Processing Map

The ultimate goal is to produce components with regulated microstructure and properties on a repeatable basis in a manufacturing environment, without macro- or microstructural defects [9]. Microstructures of deformed samples showed that under these storage conditions, dynamic recovery is the mechanism. The approach to processing maps was found to be useful in achieving optimum processing parameters and preventing microstructural defects like flow instability [22]. Figure 2 shows the processing maps for 7075 Al alloy, and 7075Al/SiCp with 5 μm, 20 μm, and 63 μm composites obtained by superimposing the instability map on the 0.5 strain efficiency is shown in Fig. 2a–d, respectively. The contour numbers represent the efficiency of power dissipation, and the shaded domains show the flow instability regions. The difference of microscopic stress and strain distributions is lower in finer microstructure composites. Temperature rises in the DRX domain as the particle size increases [23]. It is in good agreement with the findings reviewed as, Fig. 2a the map exhibits a DRX domain in the temperature range 350–395 oC and strain rate range 0.013–0.12 s^{-1} with a peak efficiency of about 28% occurring at 350 °C and 0.1 s^{-1}. In Fig. 2b, the map exhibits that the DRX domain is obtained at the temperature, and strain rate ranges are 345–385 °C and 0.01–0.1 s^{-1} with a peak efficiency of about 26% at 365 °C and 0.05 s^{-1}(5 μm). In Fig. 2c, the DRX domain occurs in the region of 355–420 °C for a strain rate range of 0.01–0.1 s^{-1}. The maximum efficiency in this domain is 44%, increasing from 20%. In Fig. 2d, the DRX domain occurs in the region of 435–495 °C for a strain rate range of 0.02–0.16 s^{-1}. The maximum efficiency in this domain is 36%(63 μm). In the 7075Al/SiCp with 20 μm composites (Fig. 2c), the maximum efficiency is due to the high bonding area when compared with the small particle size, i.e., 5 μm reinforcement size.

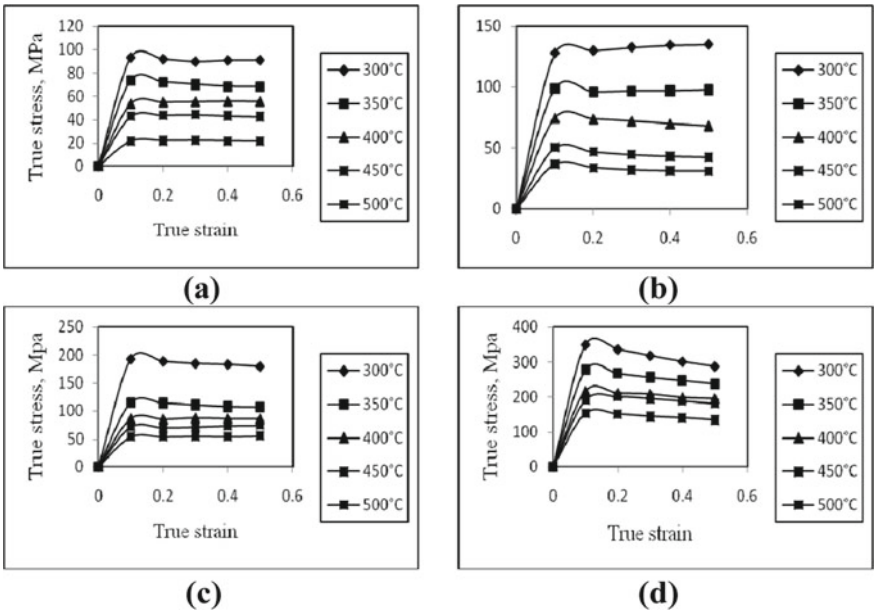

Fig. 1 **a** Flow curves of 7075 Al alloy for different temperatures at constant strain rate of 0.1 s^{-1} **b** Flow curves of 7075 Al/15%SiCp (5 μm) for different temperatures at constant strain rate of 0.1 s^{-1} **c** Flow curves of 7075 Al/15%SiCp (20 μm) for different temperatures at constant strain rate of 0.1 s^{-1} **d** Flow curves of 7075 Al/15%SiCp (63 μm) for different temperatures at constant strain rate of 0.1 s^{-1}

The stable efficiency value as a strain function indicates that the dissipation of power occurs through microstructural equilibrium processes that occur during deformation, i.e., dynamic restoration processes such as DRX and DRV. However, for verification, thorough microstructural analysis will still be required. A high efficiency in the stable environment suggests better conditions for process. Deformation efficiency of composites improves with an increase in reinforcement particle sizes up to 20 μm (5 μm—efficiency is 26%, 20 μm—efficiency is 44%), then the efficiency decreases for composites with a reinforcement particle size of 63 μm (36%), as larger particles fragment more easily during deformation than smaller ones [23].

3.3 Microstructural Examination

Interpretations of the various domains of deformation must be based on microstructural validation [22]. Figure 3a shows the micrograph of deformed 7075Al alloy at 350 °C and 0.1 s^{-1} and Fig. 3b, c deformed 7075Al/SiCp with 5 μm and 20 μm at 400 °C and 0.1 s^{-1}. Fig. 3d shows deformed 7075Al/SiCp with 63 μm at 450 °C and 0.1 s^{-1}. With wavy grain boundaries typical of grain processing by dynamic

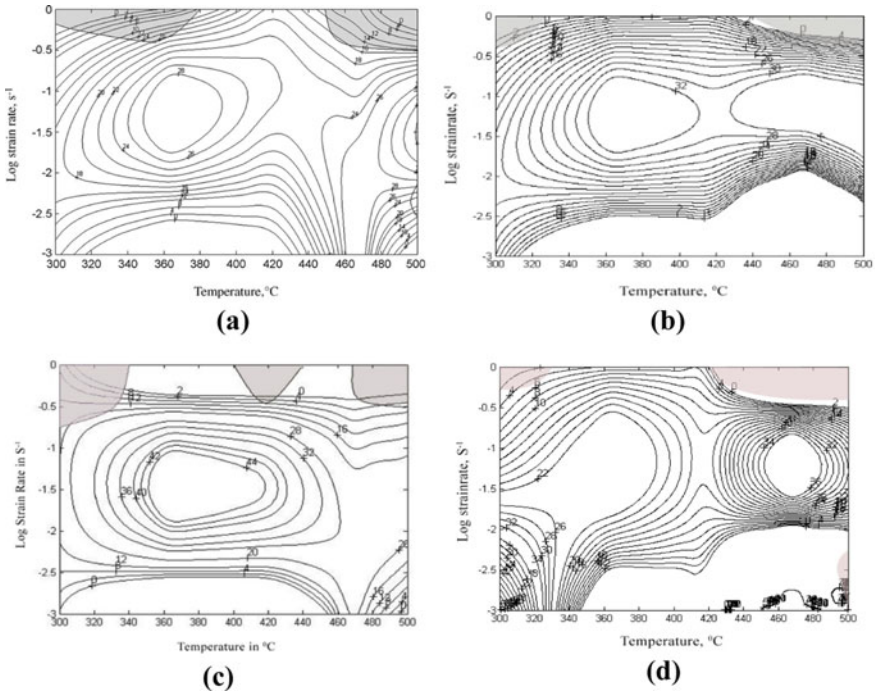

Fig. 2 **a** Processing map for 7075 alloy **b** Processing map for 7075Al/15%SiCp (5 μm) composites **c** Processing map for 7075Al/15% SiCp (20 μm) composites **d** Processing map for 7075Al/15% SiCp (63 μm) composites

recrystallization (DRX) [24], fine grains are observed in the above micrographs. The occurrence of dynamic recovery and dynamic recrystallization at higher temperatures and moderate strain rate deformation results in a significant reduction in flow stress. DRX is more successful than the DRY, however. DRX is a domain chosen to optimize hot workability and control good microstructure [24]. It is found that in the composites the dynamically recrystallized volume of grain is smaller than in alloy. This is done in the matrix by strong particles. The maximum power dissipation efficiency in the DRX domain of the 7075 Al/20 μm of SiCp is higher than that of 7075 Al alloys and 7075 Al/5 μm, 63 μm of SiCp. Large reinforcement particles are prone to fracture compared to smaller ones [25]. This particle fracture phenomenon is not expected to be an effective mechanism at high temperatures but to increase the relaxation temperature for a given strain rate for a large particle size composite reinforced lower temperature compared to temperature restoration can result in pressure accumulation at the particle/matrix interfaces. In the end, this leads to more fracture events involving the reinforcement of large particles and matrix cavitations [25, 26].

It is well agreement with the present study that particle cracking is identified in 7075Al/15% SiCp composites of higher reinforcement particle sizes (20 and 63 μm) which are as shown in Fig. 4a, b. Overall, during deformation, larger particles fracture

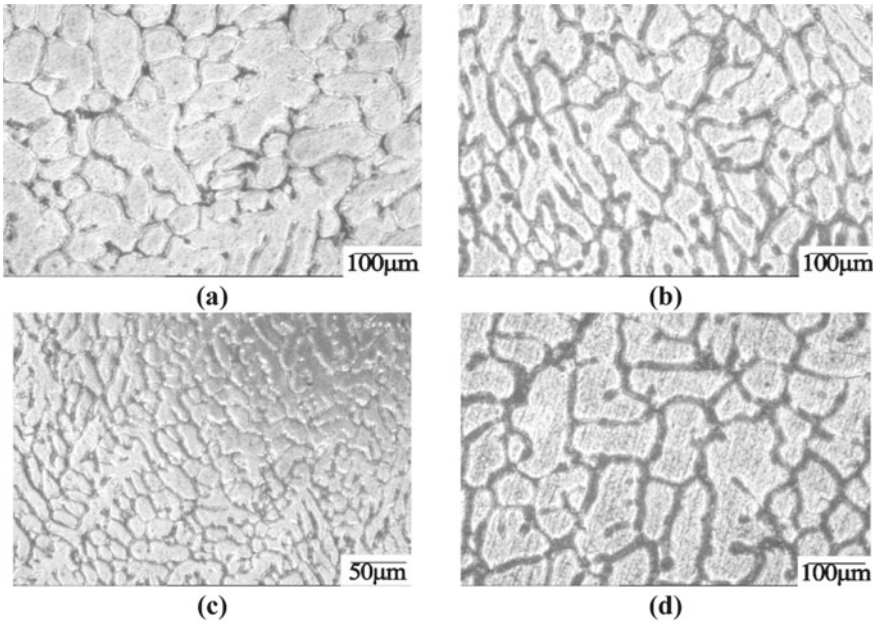

Fig. 3 **a** Dynamic recrystallization for 7075Al alloy at 350 °C at a strain rate of 0.1 s^{-1} **b** Dynamic recrystallization for 7075Al/15% SiCp (5 μm) composites at 400 °C at a strain rate of 0.1 s^{-1} **c** Dynamic recrystallization for 7075Al/15% SiCp (20 μm) composites at 400C and at a strain rate of 0.1 s^{-1} **d** Dynamic recrystallization for 7075Al/15% SiCp (63 μm) composites at 450 °C at a strain rate of 0.1 s^{-1}

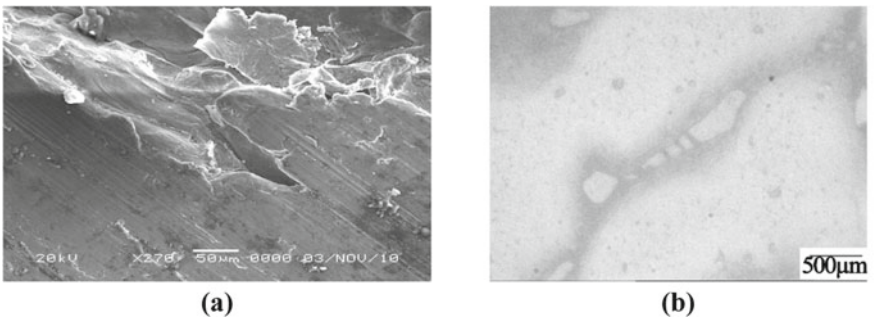

Fig. 4 **a** SEM image of particle breakage for 7075Al/15% SiCp (20 μm) composites at 400C and at a strain rate of 1.0 s^{-1} **b** Particle cracking for 7075Al/15% SiCp (63 μm) composites at 500 ∘52C and at a strain rate of 1.0 s^{-1}

more easily than smaller ones [23]. Larger particles have a larger interface area with the matrix and are therefore subject to higher concentration of stress. The force of the particle fracture is regulated by the intrinsic defects in the particle. Because the particle size of a flaw is small, larger particles are more likely to break because they are more likely to have a flaw greater than a certain critical size [27]. In addition, the composite containing large-size reinforcement particle shows more particle breakage at a higher strain rate. Srivastava et al. [20] stated that smaller particles increase the hardening of composites by plastic work, while particle/matrix interfacial decohesion does the contrary. Similarly, smaller 17 μm particle size may also result in poor workability. Large particle size with moderate volume reinforcement fraction would therefore give improved workability.

It was also pointed out that smaller particles lead to debonding of the interface, while larger ones often fractured during loading [20]. This argument is confirmed in the present investigation, i.e., debonding occurs in 7075 Al/15%SiCp (5 μm) composites as shown in Fig. 5, particle fracture occurs in7075 Al/15%SiCp (63 μm) composites. The particle size of reinforcement dominates MMC rupture, for example, cracks usually occur in particles with a dimension greater than 5 μm, whereas small particles (< 5 μm) tend to be deboned at the matrix–particle interface [28]. Matrix stress is inhomogeneous during the initial deformation stage due to the discrepancy between the particles and the matrix of the elastic modulus. In the matrix, which closes to the tip of the particles along the loading axis, high stress also develops. In the vicinity of the particles, the stress concentration is due to the stress restriction in the presence of SiC particles [29].

Due to inhomogeneity in the stress distribution, fracture and debonding occur locally at the interfaces. This can be avoided by processing the composites between reinforced particles that do not form deformation zones. It is well known in particulate-reinforced composites that debonding particle damage is easy to occur on large particles of reinforcement and difficult to occur on small particles of reinforcement. In order to consider the effect of particle size on damage, debonding damage is assumed to be controlled by a critical energy criterion for interfacial debonding of particle–matrix. The particle size is smaller, dislocation reinforcement is more

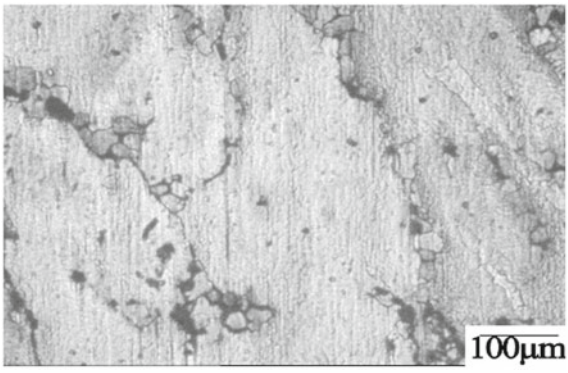

Fig. 5 Deboning for 7075Al/15% SiCp (5 μm) composites at 450 °C and at a strain rate of 1.0 s^{-1}

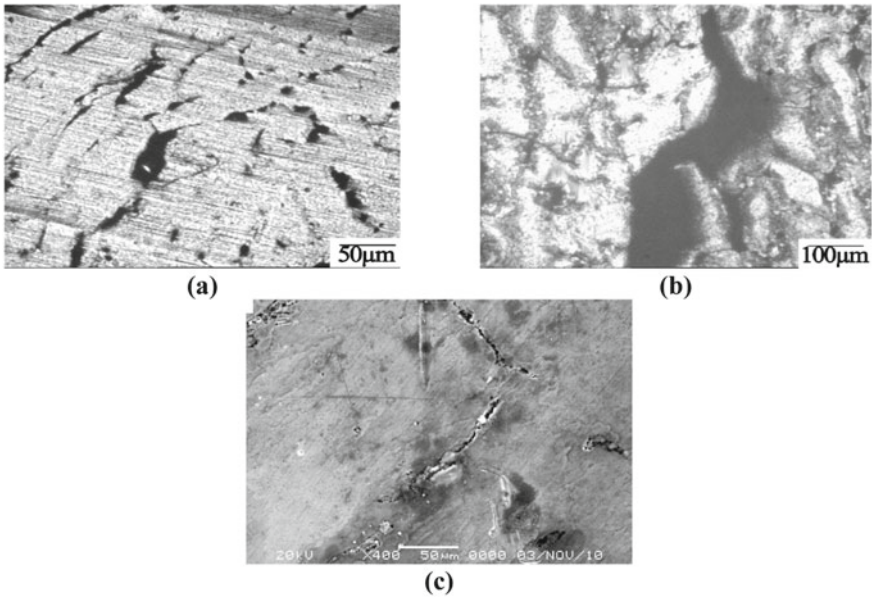

Fig. 6 **a** Matrix cracking for 7075Al/15% SiCp (5 μm) composites at 500 °C and a strain rate of 1.0 s^{-1}. **b** Interface crack for 7075Al/15% SiCp (20 μm) composites at 500C and at a strain rate of 1.0 s^{-1} **c** SEM image of interface cracking for 7075Al/15% SiCp (63 μm) composites at 500 °C and a strain rate of 1.0 s^{-1}

dominant, and debonding damage is more difficult to occur. The debonding damage occurs from larger particles to smaller particles in composites containing different sizes of particles, and the stress–strain relationship shifts to the lower side of stress [30].

The dynamic interplay of particle size, volume fraction, and strain frequency results in variability in the creation of voids and damage to particles. Low stress levels may relate large variation in the difference in porosity to the low value of matrix flow pressure, resulting in localized stress fields in turn. At a higher strain rate, high matrix flow stress does not allow large plastic strain around particles and thus fewer instances of particle breaking. At high stress frequency, particle breakage may be expected to be lower, but in such situations, the matrix cavitation phenomenon may become dominant due to inhomogeneous stress distribution in the matrix; hence matrix cracking or interface cracking may occur. Matrix cracking and interface cracking that occurs at higher strain rate and higher temperature in all the 7075Al/SiCp composite materials investigated are as shown in Fig. 6a–c.

4 Conclusions

The following conclusions were drawn from the investigation.

- Temperature rises in the DRX domain as the particle size increases. As the content of silicon carbide increases, the pore size becomes smaller, resulting in an increase in the value of the formability pressure index.
- During deformation, larger particles fracture more quickly than smaller ones. Larger particles have a wider interface with the matrix and are therefore subject to higher concentration of pressure.
- Higher reinforcement particle size of SiCp composites (7075Al (5 μm)) does not consider particle cracking. Since smaller particles improve the hardening of composites in the plastic work.
- Debonding particle damage on large reinforcement particles is easy to occur and is difficult to occur on small reinforcement particles due to the more prevalent dislocation reinforcement. Significant particle fracture and interface debonding at large strains can be related due to the low flow pressure of large particle size reinforced composites. Due to inhomogeneity in the stress distribution, fracture and debonding occur locally at the interfaces.
- Deformation efficiency of composites increases with an increase in reinforcement particle sizes up to 20 μm (5 μm—efficiency is 26%, 20 μm—efficiency is 30%), then the efficiency decreases for composites with a reinforcement particle size of 63 μm (28%)

Acknowledgements The authors thank the Department of Manufacturing Engineering, Annamalai University, Tamilnadu, India, for their support in the manufacture and testing of composites.

References

1. Zhang BL, Baker TN (2004) Effect of the heat treatment on the hot deformation behaviour of AA6082 alloy. J Mater Process Technol 153–154:881–885
2. Bardi F, Cabibbo M, Spigarelli S (2002) An Analysis of Thermo-Mechanical Treatments of A 2618 Aluminium Alloy: Study of Optimum Conditions for Warm forging". Materilas Science Engineering a 334:87–95
3. Hu HE, Zhen L, Yang L (2008) Deformation behavior and microstructure evolution of 7050 aluminum alloy during high temperature deformation. Materials Science Engineering a 488:64–71
4. Bedir F (2007) Characteristic properties of Al–Cu–SiCp and Al–Cu–B4Cp composites produced by hot pressing method under nitrogen atmosphere. Materials Design 28:1238–1244
5. Abouelmagd G (2004) Hot deformation and wear resistance of P/M aluminium metal composites. J Mater Process Technol 155–156:1395–1401
6. Kalkanl A, Yılmaz S (2008) Synthesis and characterization of aluminum alloy 7075 reinforced with silicon carbide particulates. Materials Design 29:775–780
7. Srinivasan N, Prasad YVRK, Ramarao P (2008) Hot deformation behaviour of Mg– 3A alloy a study using processing map. Mater Sci Eng, a 476:146–156

8. Liu LF, Dai LH, Yang GW (2003) Strain gradient effects on deformation strengthening behavior of particle reinforced metal matrix composites. Mater Sci Eng A 345:190–196
9. Cavaliere P, Cerri E, Leo P (2004) Hot deformation and processing maps of a particulate reinforced 2618/Al2O3/20p metal matrix composite. Compos Sci Technol 64:1287–1291
10. Prasad YVRK (2003) Processing maps—a status report, On the hot working characteristics of 2014 Al–20 vol% Al2O3 metal matrix composite. Journal of Material Engineering Performance. 12:638–645
11. Narayana Murty SVS, Nageswara Rao B, Kashyap BP (2005) On the hot working characteristics of 2014 Al–20 vol% Al2O3 metal matrix composite. J Mater Process Technol 166:279–285
12. McQueen HJ, Ryan ND (2002) Constitutive analysis in hot working. Materials Science Engineering. A 322:43–63
13. Narayana Murty SVS, Nageswara Rao B, Kashyap BP (2005) Identification of flow instabilities in the processing maps of AISI 304 stainless steel. J Mater Process Technol 166:268–278
14. Lin YC, Chen MS, Zhong J (2008) Prediction of 42CrMo steel flowstress at high temperature and strain rate. Mech Res Commun 35(3):142–150
15. Prasad YVRK, Rao KP (2005) Processing maps and rate controlling mechanisms of hot deformation of electrolytic tough pitch copper in the temperature range 300–950°C. Mater Sci Eng, a 391:141–150
16. Kouzeli M, Mortensen A (2002) Size dependent strengthening in particle reinforced aluminum. Acta Mater 50:39–51
17. Cerri E, Spigarelli S, Evangelista E, Cavaliere P (2002) Hot deformation and processing maps of a particulate-reinforced 6061+20% Al_2O_3 composite. Mater Sci Eng, a 324:157–161
18. Qu S, Siegmund T, Huang Y, Wu PD, Zhang F, Hwang K (2005) A study of particle size effect and interface fracture in aluminum alloy composite via an extended conventional theory of mechanism-based strain-gradient plasticity. Compos Sci Technol 65:1244–1253
19. Narayanasamy R, Ramesh T, Prabhakar M (2009) Effect of particle size of SiC in aluminium matrix on workability and strain hardening behaviour of P/M composite. Mater Sci Eng, a 504:13–23
20. Srivastava VC, Jindal V, Uhlenwinkel V, Bauckhage K (2008) Hot-deformation behaviour of spray-formed 2014 Al + SiCP metal matrix composites. Mater Sci Eng, a 477:86–95
21. Milan MT, Bowen P (2004) Tensile and Fracture Toughness Properties of SiCp Reinforced Al Alloys: Effects of Particle Size, Particle Volume Fraction, and Matrix Strength. the Journal of Materials Engineering and Performance. 13(6):775–783
22. Prasad YVRK, Sasidhara S (eds) (1997) Hot Working Guide: A Compendium of Processing Maps. ASM International, Materials Park, OH
23. Tham LM, Gupta M, Cheng L (2002) Effect of reinforcement volume fraction on the evolution of reinforcement size during the extrusion of Al-SiC composites. Mater Sci Eng, a 326:355–363
24. Xiao BL, Fan JZ, Tian XF, Zhang WY, Shi LK (2005) Hot deformation and processing map of 15%SiCp/2009 Al composite. J Mater Sci 40:5757–5762
25. Ferry M, Xiao Guo Z (Ed) (2005) The deformation and Processing of structural materials, Woodhead Publishing Ltd., Cambridge, England, p 203
26. Clyne TW, Withers PJ (1993) An introduction to metal matrix composites. Cambridge University Press, Cambridge
27. Wang Z, Song M, Sun C, Xiao D, He Y (2010) Effect of extrusion and particle volume fraction on the mechanical properties of SiC reinforced Al–Cu alloy composites. Mater Sci Eng, a 527:6537–6542
28. Balasivanandha Prabu S, Karunamoorthy I (2008) Microstructure-based finite element analysis of failure prediction in particle-reinforced metal matrix composite. J Mater Process Technol 207(1/3):53−62
29. Peng Z (2010) Li fu-guo, "Effect of particle characteristics on deformation of particle reinforced metal matrix composites." Transactions of Nonferrous Metals Society of China 20:655–661
30. Tohgo K, Itoh Y, Shimamura Y (2010) A constitutive model of particulate-reinforced composites taking account of particle size effects and damage evolution. Composites: Part A 41(2):313–321